Appl. Phys. B 87, 731–737 (2007)
DOI: 10.1007/s00340-007-2650-6

Applied Physics B
Lasers and Optics

N. CHAI[1]
S.V. NAIK[1]
W.D. KULATILAKA[1]
N.M. LAURENDEAU[1]
R.P. LUCHT[1,✉]
S. ROY[2]
J.R. GORD[3]

Detection of acetylene by electronic resonance-enhanced coherent anti-Stokes Raman scattering

[1] School of Mechanical Engineering, Purdue University, West Lafayette, IN 47907, USA
[2] Innovative Scientific Solutions, Inc., 2766 Indian Ripple Road, Dayton, OH 45440, USA
[3] Air Force Research Laboratory, Propulsion Directorate, Wright-Patterson AFB, OH 45433, USA

Received: 30 November 2006/Revised version: 5 March 2007
Published online: 16 May 2007 •

ABSTRACT We report the detection of acetylene (C_2H_2) at low concentrations by electronic resonance-enhanced coherent anti-Stokes Raman scattering (ERE-CARS). Visible pump and Stokes beams are tuned into resonance with Q-branch transitions in the v_2 Raman band of acetylene. An ultraviolet probe beam is tuned into resonance with the $\tilde{A}$–$\tilde{X}$ electronic transition of C_2H_2, resulting in significant electronic resonance enhancement of the CARS signal. The signal is found to increase significantly with rising pressure for the pressure range 0.1–8 bar at 300 K. Collisional narrowing of the spectra appears to be important at 2 bar and above. A detection limit of approximately 25 ppm at 300 K and 1 bar is achieved for our experimental conditions. The signal magnitudes and the shape of the C_2H_2 spectrum are essentially constant for UV probe wavelengths from 233.0 to 238.5 nm, thus indicating that significant resonant enhancement is achieved even without tuning the probe beam into resonance with a specific electronic resonance transition.

PACS 42.65.Dr; 42.62.Fi; 42.65.-k

1 Introduction

Coherent anti-Stokes Raman scattering (CARS) is a useful and accurate technique for performing spatially resolved measurements of temperature and major-species concentrations [1, 2]. CARS can be used for simultaneous measurement of multiple species concentrations and temperature in a single laser shot when using appropriate broadband laser sources [3]. The detection limit for CARS is typically 1000 ppm or greater at atmospheric pressure [1], even for well-optimized CARS systems with polarization background subtraction.

Electronic resonance-enhanced (ERE) CARS was first demonstrated for dilute solutions of diphenyloctatetraene in benzene [4]. Several molecules and radicals have been investigated via ERE-CARS including I_2 [5, 6], NO_2 [7, 8], C_2 [9–11], S-tetrazine vapor [12], OH [13], and CH [14]. Hanna et al. [15] demonstrated ERE-CARS for nitric oxide (NO) by implementing a dual-pump CARS approach and observed significant resonance enhancement. Kulatilaka et al. [16] employed ERE-CARS to monitor NO concentrations in a combustion environment. A detection limit of approximately 50 ppm was demonstrated in a hydrogen-air flame, thus confirming the utility of ERE-CARS for measurements of minor species in reacting flows. Kulatilaka et al. [17] subsequently investigated pressure-scaling and saturation effects for NO ERE-CARS. The ERE-CARS signal for NO was found to increase with rising pressure up to 2 bar and to remain nearly constant thereafter up to 8 bar.

Measurements of acetylene (C_2H_2) concentration are important for understanding many combustion processes. Acetylene plays an important role in the chemical kinetics of both soot initiation and growth [18, 19], and also in the formation of polycyclic aromatic hydrocarbons [19]. Measurements of acetylene, moreover, are useful for understanding surface chemistry related to chemical vapor deposition as well as to carbon-nanotube synthesis via combustion [20].

2 Experimental description

The energy-level diagram for the C_2H_2 ERE-CARS process is shown in Fig. 1. The frequency difference between the pump beam at a vacuum wavelength $\lambda_1 = 532.215\,\text{nm}$ ($18\,789.4\,\text{cm}^{-1}$) and the Stokes beam at $\lambda_2 \cong 594\,\text{nm}$ ($16\,815\,\text{cm}^{-1}$) corresponds to a Raman shift of $1974\,\text{cm}^{-1}$ – the frequency of the bandhead for the v_2 band of acetylene. The Raman polarization induced in the medium is detected using an ultraviolet (UV) probe beam at $\lambda_3 \cong 236\,\text{nm}$ ($42\,370\,\text{cm}^{-1}$). The ERE-CARS signal is near resonance with various ro-vibrational bands in the $\tilde{A}$–$\tilde{X}$ electronic transition of C_2H_2 [21–23], and has a wavelength $\lambda_{CARS} \cong 225.5\,\text{nm}$ ($44\,350\,\text{cm}^{-1}$). Acetylene is a linear molecule in its ground electronic state with five fundamental vibrations [24], and has a planar trans-bent geometry in its lowest excited singlet state [21]. Among five fundamental vibrations in the ground electronic state, three are Raman-active; the other two are infrared-active. The v_2 band at $1974\,\text{cm}^{-1}$ corresponds to symmetric stretching of the molecule and is the strongest of the three Raman-active modes [24]. The complete v_2 Raman band of acetylene can be acquired by scanning λ_2 for fixed λ_1 and λ_3.

✉ Fax: +1-765-494-0539, E-mail: lucht@ecn.purdue.edu

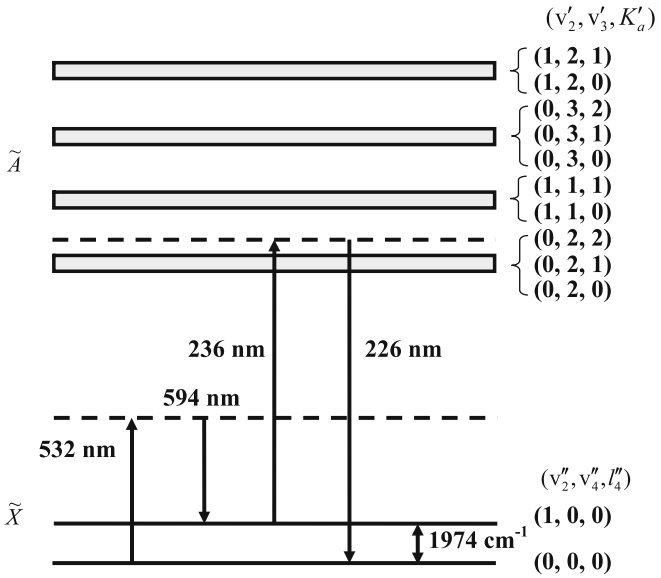

FIGURE 1 Energy-level diagram for the C_2H_2 ERE-CARS process

2.1 *Optical system*

The experimental apparatus for our C_2H_2 ERE-CARS measurements is shown in Fig. 2. The second-harmonic output of an injection-seeded, Q-switched Nd:YAG laser (Spectra-Physics Model Quanta Ray PRO 290-10) is split via a 90/10 beam splitter. Ninety percent of the second-harmonic beam is employed to pump a tunable, narrowband dye laser (Continuum Model ND 6000), which produces an output beam at a wavelength of approximately 704 nm. LDS 698 laser dye is used within the ND 6000 dye laser. The remaining 10% of the second-harmonic beam is used as the pump beam (ω_1). The repetition rate of the laser is 10 Hz, and the temporal pulse length is approximately 8 ns at full-width at half-maximum (FWHM).

The third-harmonic output at 355 nm of the same injection-seeded Spectra-Physics Nd:YAG laser is sum-frequency mixed with the Continuum dye-laser output at 704 nm, generating a tunable UV probe beam (ω_3) at 236 nm. A beta-barium-borate (β-BBO) crystal mounted in an Inrad Autotracker III is used for the sum-frequency mixing process. This tunable UV source, whose maximum energy is ~ 4 mJ/pulse, constitutes the probe beam (λ_3). Finally, the second-harmonic output of an unseeded Nd:YAG laser (Continuum Model Precision PRO 9010) is used to pump another tunable, narrowband dye laser (Lumonics Model SpectrumMaster). Rhodamine 610 laser dye is employed to generate the Stokes beam (ω_2) near 594 nm.

The two Nd:YAG lasers are synchronized using a digital delay generator (SRS Model DG 535) so that all three beams overlap temporally with a peak deviation of less than 1 ns. A combination of a half-wave plate and a polarizer is placed within each beam path to control the pulse energy. The polarizer is also used to set the desired polarization for each beam. The pump beam and the Stokes beam are linearly polarized, with the polarization axis set at 60° with respect to the vertical axis. The UV probe beam is vertically polarized. A three-dimensional folded BOXCARS geometry is employed to satisfy the phase-matching requirement [25].

A 50-mm diameter, 500-mm focal-length, UV-grade fused-silica lens is used to focus the three beams. However, to obtain better signal-to-noise ratios while maintaining reasonable spatial resolution, the beams are overlapped about 25 mm away from their focal plane. This spatial overlap also reduces saturation effects for both the Raman and electronic transitions [12] because of reduced laser irradiances at the probe volume. The length of the resulting probe volume is about 6 mm. The diameters of all three beams at the probe volume are approximately 200 μm, as measured by translating a razor blade across the overlap region while monitoring the transmitted power of each laser.

The three input beams and the signal beam are recollimated using another 50-mm diameter, 500-mm focal-length lens. The Stokes beam (λ_2) is directed into a wavemeter (High Finesse Model WS-6) to record its wavelength when scanning the Stokes dye laser. The pump beam (λ_1) is trapped using a beam dump. The UV probe beam (λ_3) is directed onto a pyroelectric joulemeter (Molectron Model J3-05). The UV probe pulse energy is recorded continuously so that shot-to-shot fluctuations in the UV-beam energy can be accounted for in subsequent data analysis.

The ERE-CARS signal and the non-resonant four-wave-mixing signal are directed through an analyzing polarizer of high rejection ratio. The transmission axis of the analyzer is set perpendicular to the polarization direction of the non-resonant signal, thus minimizing non-resonant interferences. The analyzing polarizer is mounted on a high-resolution rotation stage to achieve the best possible suppression of non-resonant background. Light scattered from the UV beam at 236 nm is blocked using four band-pass filters [15], as shown in Fig. 2. The signal beam at ~ 225.5 nm is isolated using a 1-m spectrometer (SPEX Model 1000M) and collected via a solar-blind photomultiplier tube (PMT-Hamamatsu Model R7154).

2.2 *Flow and pressure systems*

For measurements of the detection limit, we employ a jet flow of acetylene in a buffer gas of nitrogen. Molecular mixing is ensured by combining a gas flow of 1000 ppm C_2H_2 in N_2 with an additional flow of pure N_2 sufficiently far upstream of the nozzle. The diameter of the nozzle producing the jet flow is approximately 10 mm. Careful adjustments are made to ensure that the probe volume is completely encompassed by the jet.

The pressure-scaling experiments are performed in a pressure vessel which can accommodate pressures up to 8 bar. The inlet of the vessel is connected to a gas bottle containing 1000 ppm C_2H_2 in N_2. In addition, the outlet of the vessel is connected to a vacuum pump. It is ensured that no residual mixture remained in the vessel prior to refilling of the vessel at each pressure.

3 Results and discussion

The ERE-CARS signal is acquired while scanning the frequency of the Stokes dye laser and fixing that of the UV probe beam. In past ERE-CARS measurements of nitric oxide [15, 16], we have performed both UV scans (λ_2 fixed, λ_3 varying) and Stokes scans (λ_2 varying, λ_3 fixed). However,

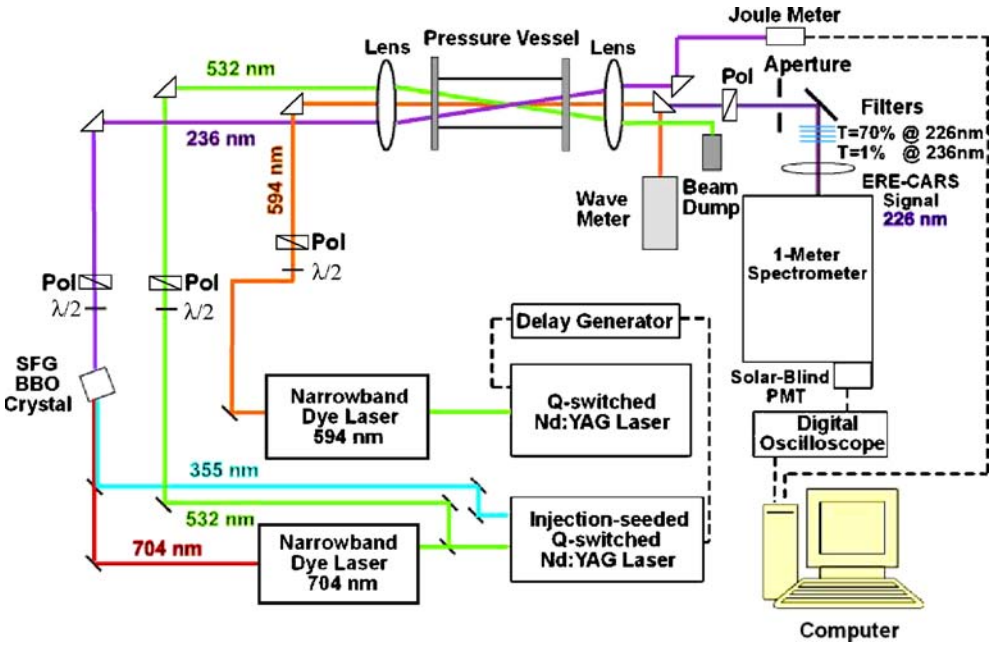

FIGURE 2 Experimental system for C_2H_2 ERE-CARS

for this work, we present only Stokes scans. UV scans are performed but yield essentially constant signals owing to the broad character of the electronic resonance interaction. The ERE-CARS signal is averaged over 10 laser shots and subsequently corrected for shot-to-shot UV (λ_3) fluctuations via division by the UV energy. It is observed that the fluctuations in the Stokes laser beam (λ_2) are negligible.

Spectral v_2 band structures for 1% C_2H_2 at 0.05 atm and 300 K for various pulse energies of both the pump beam (ω_1) and Stokes beam (ω_2) are shown in Figs. 3 and 4. The Sandia CARSFT code [26] is used to calculate theoretical CARS spectra for given laser linewidths at the specified temperature and pressure. The CARSFT calculations do not include any effects of saturation. Figure 3 shows a comparison between theoretical and measured spectra for the same experimental conditions at fixed energy levels for ω_1 and ω_2. Good agreement is achieved between theory and experiment. The remaining differences between theory and experiment are probably due to slight saturation of the experimental spectrum. The odd rotational lines are well resolved in Fig. 3, but the even rotational lines are not evident. The linewidth (FWHM) of the pump beam (λ_1) is $\sim 0.003\,\mathrm{cm}^{-1}$; in comparison, that of both the Stokes beam (λ_2) and the UV probe beam (λ_3) is approximately $0.1\,\mathrm{cm}^{-1}$. From Fig. 3, we observe that the odd rotational lines have FWHMs of approximately $0.1\,\mathrm{cm}^{-1}$. By comparing the two cases in Fig. 4, we find clear evidence

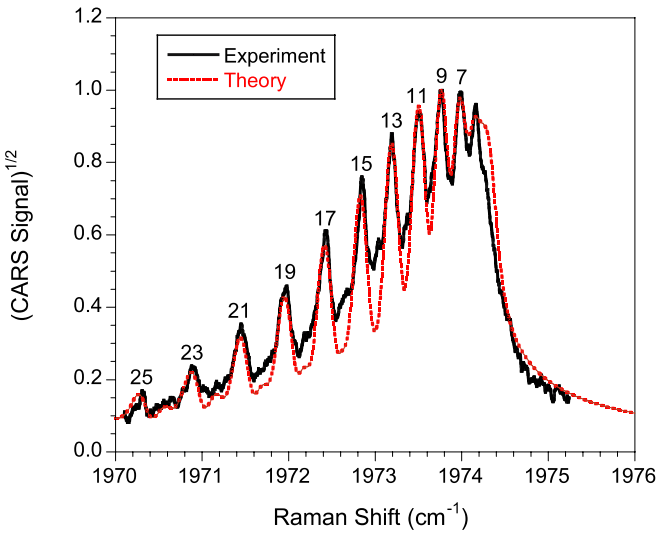

FIGURE 3 Comparison between experimental and theoretical C_2H_2 ERE-CARS spectra for 1% C_2H_2 in buffer N_2 gas at 0.05 bar and 300 K. The experimental spectrum is obtained for pulse energies of 2 mJ/pulse, 2 mJ/pulse, and 0.5 mJ/pulse for the pump, Stokes, and probe beams, respectively. The theoretical linewidths are $0.01\,\mathrm{cm}^{-1}$ and $0.15\,\mathrm{cm}^{-1}$ for the pump and Stokes beams, respectively. The Q-branch lines with odd rotational quantum number $J \geq 7$ are labeled

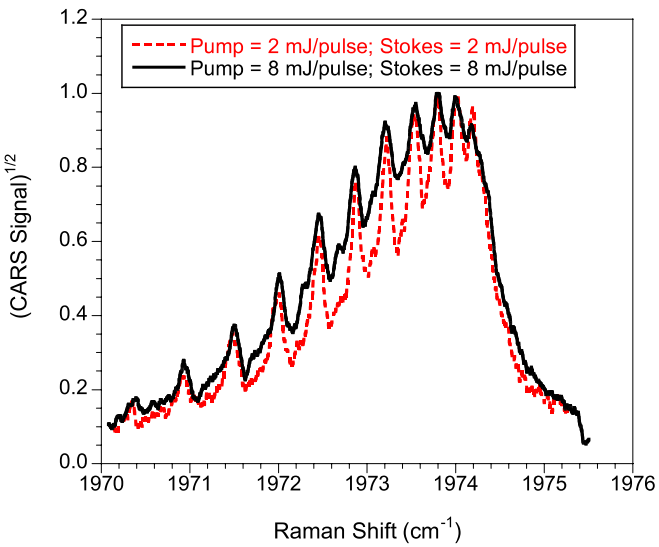

FIGURE 4 Saturation broadening of C_2H_2 ERE-CARS spectra at 0.05 bar and 300 K for 1% C_2H_2 in N_2. The pulse energy of the UV probe beam (ω_3) is 0.5 mJ/pulse for both measurements

for saturation broadening of the Raman resonances at higher pump and Stokes laser irradiances.

Figure 5 shows a comparison of theoretical and experimental ERE-CARS spectra of C_2H_2 for the v_2 Raman band at various UV probe wavelengths from 233.0 nm to 238.5 nm. From Fig. 5, we observe no significant change in the ERE-CARS spectrum as a function of UV wavelengths. The ro-vibrational structure of the acetylene $\tilde{A}$–$\tilde{X}$ electronic transition is discussed in detail by Innes [21] and Watson et al. [22]. The initial and final levels of the fundamental Q-branch transition at 1974 cm^{-1} are characterized by $(v_2'' = 0, v_4'' = 0, l_4'' = 0)$ and $(v_2'' = 1, v_4'' = 0, l_4'' = 0)$, respectively. Watson et al. [22] and Innes [21] list the frequencies and the approximate transition strengths between the $(v_2'' = 0, v_4'' = 0, l_4'' = 0)$ band in the $\tilde{X}$ level and various vibrational bands in the $\tilde{A}$ level. The bands in the $\tilde{A}$ level that are connected with the ground $(v_2'' = 0, v_4'' = 0, l_4'' = 0)$ band are listed in Table 1. The band frequency, strength (S = strong, M = medium, W = weak, VW = very weak), and corresponding UV probe wavelength are listed for exact resonance with a given band. Neither Watson et al. [22] nor Innes [21] provide any information on transitions from the $(v_2'' = 1, v_4'' = 0, l_4'' = 0)$ band in the $\tilde{X}$ level.

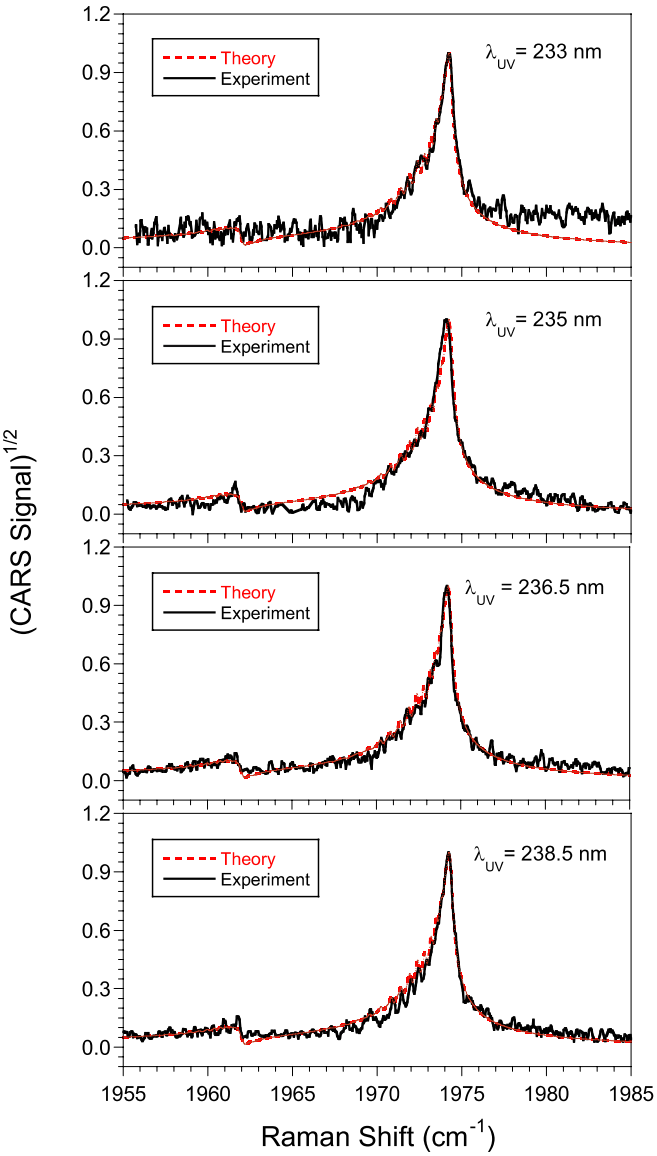

FIGURE 5 C_2H_2 ERE-CARS spectra at 1.0 atm and 300 K in a jet flow of 1% C_2H_2 in buffer N_2. The UV probe wavelength varies from 233.0 nm to 238.5 nm

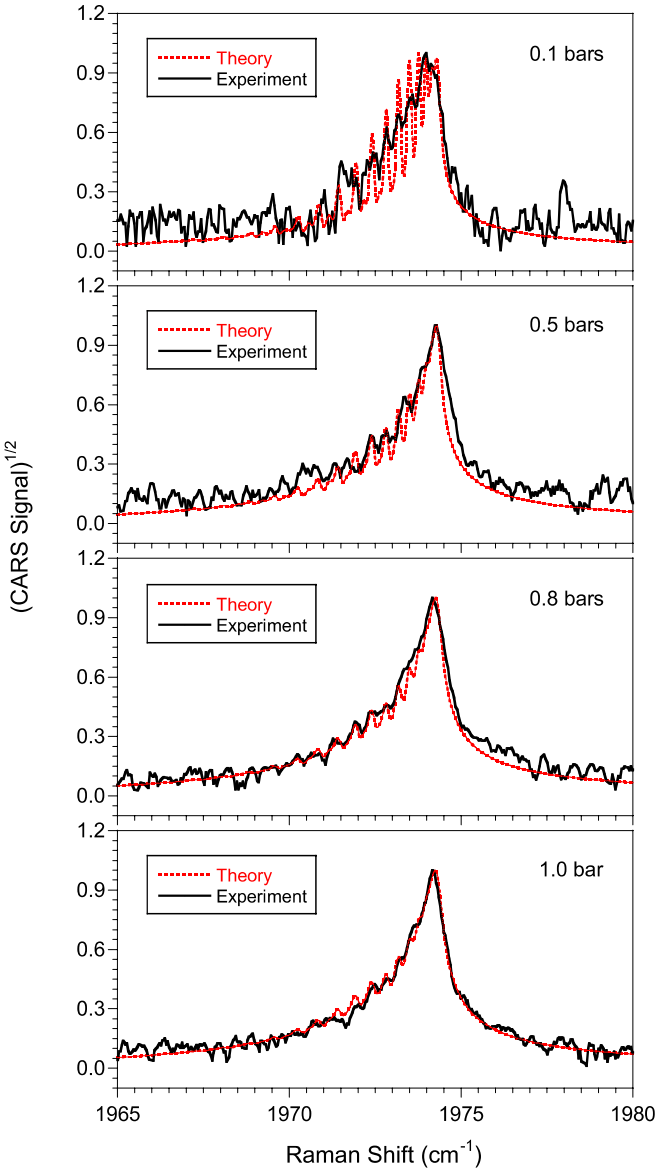

FIGURE 6 C_2H_2 ERE-CARS spectra at four different sub-atmospheric pressures. The spectra are recorded for a mixture of 1000 ppm C_2H_2 in N_2 buffer gas inside the pressure vessel. For all spectra, the UV probe wavelength $\lambda_3 = 236$ nm. The pulse energies for the pump, Stokes, and probe beams are 8.0, 8.0, and 0.5 mJ/pulse, respectively

Although it appears from Table 1 that we should have observed a significant increase in signal for $\lambda_3 = 236.5$ nm as compared to the other probe wavelengths investigated, no significant change is observed in the ERE-CARS spectrum. In fact, the maximum signal strength is found near 236 nm, so that most of the measurements reported in this paper are obtained with a probe wavelength of 236 nm.

ERE-CARS measurements for the v_2 Raman band of C_2H_2 are also performed for pressures ranging from sub-atmospheric (0.1 bar) to above atmospheric (8 bar) at 300 K. Figure 6 shows comparisons between theoretical and experimental spectra at different sub-atmospheric pressures from

0.1 to 1 bar, while Fig. 7 shows similar comparisons at pressures from 2 to 8 bar. We find, as expected, that individual rotational lines blend into a band structure as the pressure rises. In general, the theoretical and experimental spectra agree well for pressures less than 2 bar. The experimental spectrum at 0.1 bar is not as clearly resolved as the theoretical spectrum. This result is almost certainly due to the higher level of saturation for the Raman transitions at lower pressure. For pressures higher than 1 bar, the experimental spectra are narrower than the theoretical spectra. This trend becomes more pronounced at higher pressures. The implication is that significant collisional narrowing occurs at pressures above 2 bar; unfortunately, the CARSFT code does not include a collisional narrowing model for C_2H_2. The experimental spectra tend to be more symmetric at higher pressures as compared with the theoretical spectra, again presumably due to strong collisional narrowing.

$\tilde{A}$ band (v'_2, v'_3, K'_a)	$\tilde{\nu}$ (cm^{-1})	Strength	λ_3 (nm)
(0, 1, 0)	43 245.12	S	242.30
(0, 1, 1)	43 258.05	S	242.22
(0, 1, 2)	43 296.75	W	242.00
(0, 1, 3)	43 360.94	VW	241.62
(1, 0, 0)	43 584.45	W	240.32
(1, 0, 1)	43 596.31	M	240.26
(0, 2, 0)	44 275.27	M	236.40
(0, 2, 1)	44 289.35	S	236.32
(0, 2, 2)	44 331.40	W	236.09
(1, 1, 0)	44 631.78	M	234.42
(1, 1, 1)	44 644.45	M	234.35
(0, 3, 0)	45 285.72	S	230.88
(0, 3, 1)	45 301.13	S	230.80
(0, 3, 2)	45 347.15	M	230.56
(1, 2, 0)	45 662.68	M	228.89
(1, 2, 1)	45 676.42	S	228.82

TABLE 1 Bands in the $\tilde{A}$ level connected with the ($v''_2 = 0$, $v''_4 = 0$, $l''_4 = 0$) band in the $\tilde{X}$ level

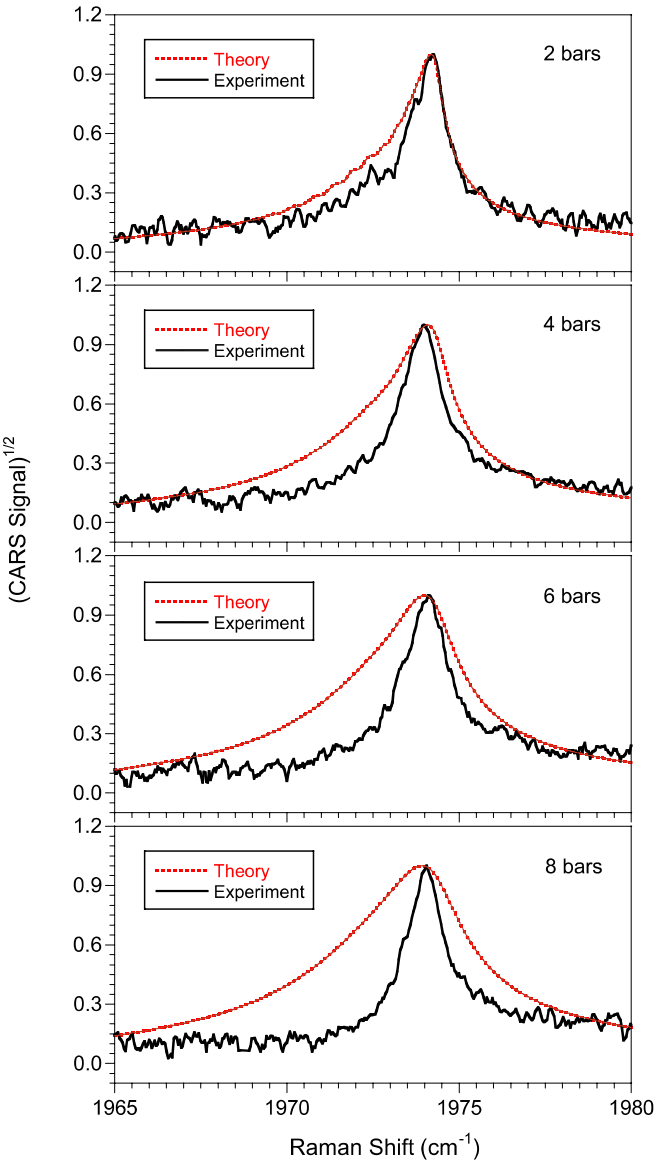

FIGURE 7 C_2H_2 ERE-CARS spectra at pressures from 2 to 8 bar. All spectra are recorded for a mixture of 1000 ppm C_2H_2 in N_2 buffer gas inside the pressure vessel. The UV probe wavelength λ_3 and the pulse energies are the same as for Fig. 6

For the spectra shown in Figs. 6 and 7, the square root of the ERE-CARS signal is integrated in the Raman shift range from 1970 cm^{-1} to 1978 cm^{-1} and plotted as a function of pressure in Fig. 8. Figure 8 shows that the square root of the integrated ERE-CARS signal increases sharply with increasing pressure from 0.1 to 4 bar and then increases gradually beyond 5 bar. The spectral scans are repeated at pressures of 1, 4, 5, and 7 bar. From these repeated measurements, we conclude that the square root of the integrated ERE-CARS signal is repeatable to within 5%. Baum et al. [27] performed acetylene absorption measurements in the wavelength range 189–229 nm for a path length of 127 mm. They found that the absorbance near 226 nm is negligibly small at 1 atm for a C_2H_2 concentration of 630 ppm. Therefore, despite changes in number density and the effects of line broadening, we conclude that the effects of UV absorption can be neglected for our experiments up to 8 bar.

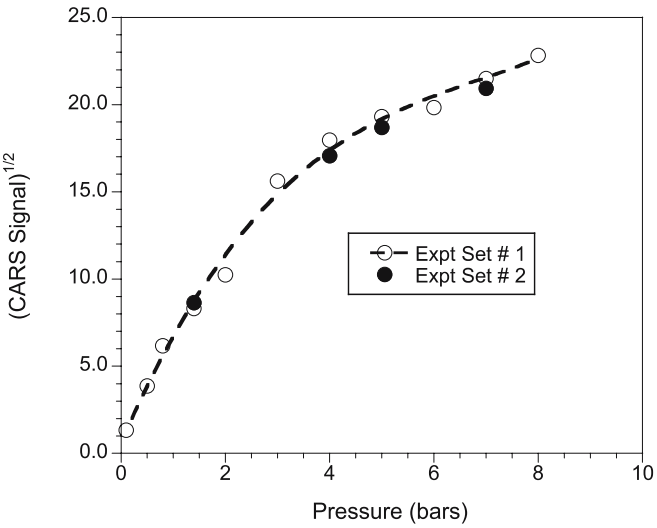

FIGURE 8 Variation of the square root of the integrated C_2H_2 ERE-CARS signal with increasing pressure in the pressure range 0.05–8 bar

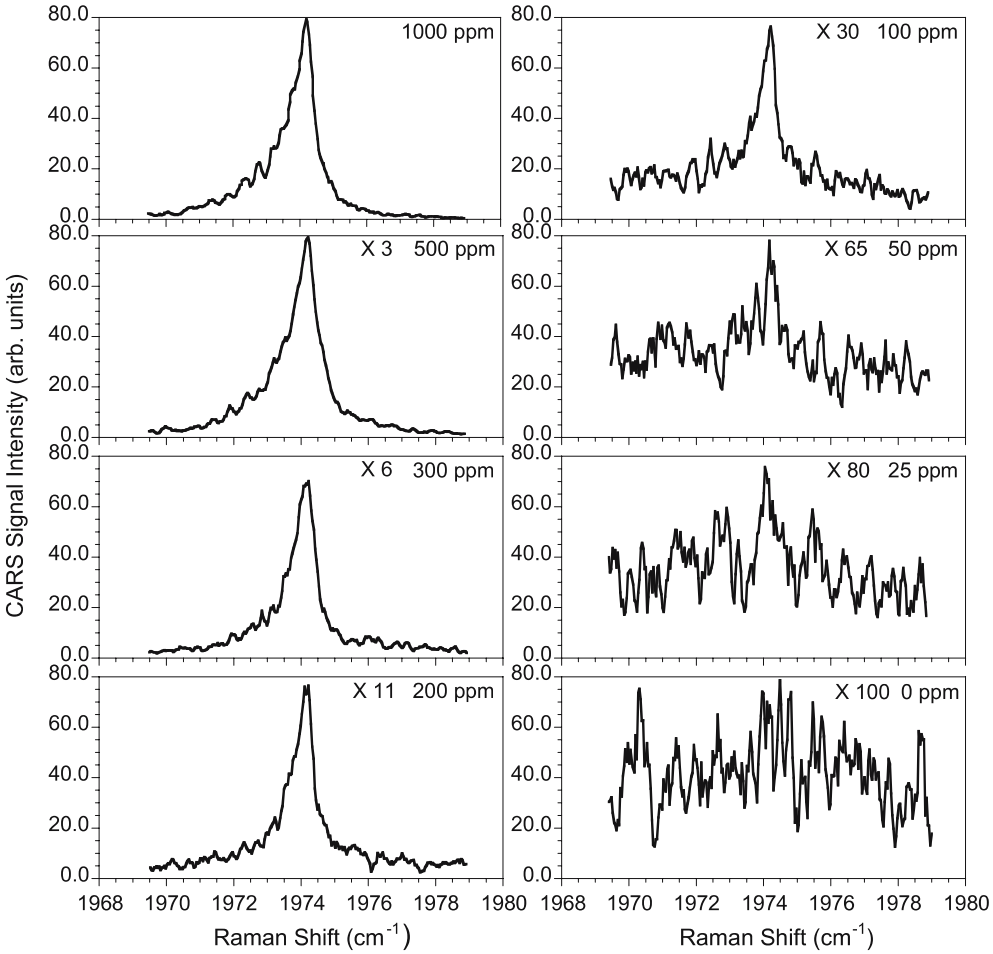

FIGURE 9 C_2H_2 ERE-CARS detection-limit measurements at 1 atm and 300 K in a jet flow of 1000 ppm C_2H_2 in N_2 buffer gas, diluted with additional N_2. For all spectra, the pulse energies for the pump, Stokes, and probe beams are 8, 8, and 2 mJ/pulse, respectively. The probe wavelength is 236.0 nm

As mentioned previously, acetylene displays an essentially constant electronic coupling with the ($v_2'' = 1$, $v_4'' = 0$, $l_4'' = 0$) level in the ground electronic state, thus yielding nearly the same resonance enhancement in the pressure range 0.1–8 bar. This factor, combined with strong collisional narrowing at high pressures, results in a substantial increase in the ERE-CARS signal with rising pressures for a constant mole fraction of C_2H_2. The gradual increase in square root of the integrated ERE-CARS signal beyond 5 bar is presumably due to broadening of the Raman transitions at higher pressures.

As indicated previously, the detection limit for CARS can be improved by several orders of magnitude by tuning the UV laser beam to a suitable electronic resonance. Figure 9 shows ERE-CARS spectra over the v_2 Raman band for different C_2H_2 concentrations. A mixture of 1000 ppm C_2H_2 in N_2 buffer gas is diluted with additional N_2 to establish the given concentration levels. The measurements are performed in a jet flow produced from a nozzle. We established a C_2H_2 detection limit of 25 ppm upon suppressing the non-resonant signal from the N_2 buffer gas. This result suggests that ERE-CARS has excellent potential for minor-species measurements, even in reacting flows.

Figure 10 shows that the square root of the integrated ERE-CARS signal (1970 cm^{-1}–1978 cm^{-1}) varies linearly with acetylene concentration at atmospheric pressure. This result verifies the expected theoretical behavior, as indicated by $I_{CARS} \propto \left|\chi^{(3)}\right|^2$, where I_{CARS} is the irradiance of the CARS signal and $\chi^{(3)}$ is the third-order nonlinear susceptibility [4].

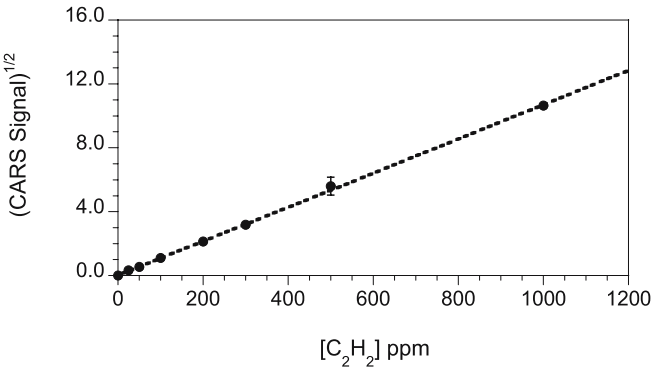

FIGURE 10 Square root of integrated C_2H_2 ERE-CARS signal as a function of C_2H_2 concentration in a jet flow at 1 atm. A typical error bar of 10% is shown at a concentration of 500 ppm

4 Conclusions and future work

Electronic resonance-enhanced coherent anti-Stokes Raman scattering (ERE-CARS) has been applied to obtain acetylene spectra at pressures ranging from 0.1 to 8 bar.

The acetylene ERE-CARS signal is found to rise sharply with increasing pressure from 0.1 to 4 bar, but more gradually from 5 to 8 bar. As expected, the square root of the integrated ERE-CARS signal at 1 atm and 300 K varies linearly with C_2H_2 concentration. The detection limit under these conditions is found to be approximately 25 ppm. No significant changes in spectral signature or signal levels are observed as the UV probe wavelength is varied from 233.0 to 238.5 nm.

We plan to apply ERE-CARS for measurement of C_2H_2 profiles in high-pressure counter-flow diffusion flames in the Purdue high-pressure flame facility [28]. Quantitative analysis of these profiles will require either calibration or the incorporation of a collisional narrowing model [29–31] for C_2H_2 in the CARSFT code.

ACKNOWLEDGEMENTS Funding for this research program was provided by the U.S. Department of Energy, Division of Chemical Sciences, Geosciences, and Biosciences, under Grant No. DE-FG02-03ER15391, by the Air Force Office of Scientific Research under Contract No. FA9550-05-C-0096 (Dr. Julian Tishkoff, Program Manager), and by the Air Force Research Laboratory, Propulsion Directorate, Wright-Patterson Air Force Base, under Contract No. F33615-03-D-2329.

REFERENCES

1 A.C. Eckbreth, *Laser Diagnostics for Combustion Temperature and Species* (Gordon and Breach Publishers, Amsterdam, 1996)
2 A.C. Eckbreth, G.M. Dobbs, J.H. Stufflebeam, P.A. Tellex, Appl. Opt. **23**, 1328 (1984)
3 R.P. Lucht, Opt. Lett. **12**, 78 (1987)
4 B. Hudson, W. Hetherington III, S. Cramer, I. Chabay, G.K. Klauminzer, Proc. Nat. Acad. Sci. **73**, 3798 (1976)
5 B. Attal, O.O. Schnepp, J.-P.E. Taran, Opt. Commun. **24**, 77 (1978)
6 A. Beckman, H. Fietz, P. Baierl, W. Kiefer, Chem. Phys. Lett. **86**, 140 (1982)
7 D.M. Guthals, K.P. Gross, J.W. Nibler, J. Chem. Phys. **70**, 2393 (1979)
8 M.E. McIlwain, J.C. Hindman, J. Chem. Phys. **73**, 68 (1980)
9 K.P. Gross, D.M. Guthals, J.W. Nibler, J. Chem. Phys. **70**, 4673 (1979)
10 W.M. Hetherington III, G.M. Korenowski, K.B. Eisenthal, Chem. Phys. Lett. **77**, 275 (1981)
11 D.A. Greenhalgh, Appl. Opt. **22**, 1128 (1983)
12 T.J. Aartsma, W.H. Hesselink, D.A. Wiersma, Chem. Phys. Lett. **71**, 424 (1980)
13 B. Attal-Trétout, S.C. Schmidt, E. Crété, P. Dumas, J.P. Taran, J. Quantum Spectrosc. Radiat. Transf. **43**, 351 (1990)
14 T. Doerk, P. Jauernik, S. Hadrich, B. Pfelzer, J. Uhlenbusch, Opt. Commun. **118**, 637 (1995)
15 S.F. Hanna, W.D. Kulatilaka, Z. Arp, T. Opatrny, M.O. Scully, J.P. Kuehner, R.P. Lucht, Appl. Phys. Lett. **83**, 1887 (2003)
16 W.D. Kulatilaka, N. Chai, S.V. Naik, N.M. Laurendeau, R.P. Lucht, J.P. Kuehner, S. Roy, J.R. Gord, Opt. Lett. **31**, 3357 (2006)
17 W.D. Kulatilaka, N. Chai, S.V. Naik, N.M. Laurendeau, R.P. Lucht, J.P. Kuehner, S. Roy, J.R. Gord, Opt. Commun. **274**, 441 (2007)
18 I. Glassman, Proc. Combust. Inst. **22**, 295 (1988)
19 H. Richter, J.B. Howard, Prog. Energ. Combust. Sci. **26**, 565 (2000)
20 J.M. Bonard, M. Croci, C. Klinke, F. Conus, I. Arfaoui, T. Stöckli, A. Chatelain, Phys. Rev. B **67**, 085 412 (2003)
21 K.K. Innes, J. Chem. Phys. **22**, 863 (1954)
22 J.K.G. Watson, M. Herman, J.C. Van Craen, R. Colin, J. Mol. Spectrosc. **95**, 101 (1982)
23 B.A. Williams, J.W. Fleming, Appl. Phys. B **75**, 883 (2002)
24 R.P. Lucht, R.L. Farrow, R.E. Palmer, Combust. Sci. Technol. **45**, 261 (1986)
25 A.C. Eckbreth, Appl. Phys. Lett. **32**, 421 (1978)
26 R.E. Palmer, The CARSFT Computer Code For Calculating Coherent Anti-Stokes Raman Spectra: User and Programmer Information, Sandia National Laboratories Report SAND89-8206, Livermore, CA (1989)
27 M.M. Baum, S. Kumar, A.M. Lappas, P.D. Wagner, Rev. Sci. Instrum. **74**, 3104 (2003)
28 C.D. Carter, G.B. King, N.M. Laurendeau, Rev. Sci. Instrum. **60**, 2606 (1989)
29 R.G. Gordon, R.P. McGinnis, J. Chem. Phys. **49**, 2455 (1968)
30 R.G. Gordon, R.P. McGinnis, J. Chem. Phys. **55**, 4898 (1971)
31 M.L. Koszykowski, R.L. Farrow, R.E. Palmer, Opt. Lett. **10**, 478 (1985)